SUPPORTING INFORMATION

Nanomolar small-molecule detection using a genetically encoded ^{129}Xe NMR contrast agent

Benjamin W. Roose, Serge D. Zemerov, Ivan J. Dmochowski*

Department of Chemistry, University of Pennsylvania, 231 South 34th St., Philadelphia, PA 19104-6323

CONTENTS

Experimental Procedures:

MBP expression and purification. MBP was expressed from the pET His6 MBP TEV LIC cloning vector, a gift from Scott Gradia acquired via Addgene (plasmid #29656). The MBP vector was transformed into BL21(DE3) competent *E. coli* cells (New England Biolabs) and grown in 6 x 1 L of LB media supplemented with 50 μg/mL kanamycin to a OD_{600} of ~1. MBP expression was induced by adding isopropyl-β-D-thiogalactopyranoside (IPTG) to a final concentration of 1 mM. The induced cells were incubated overnight at 18 °C, harvested by centrifugation, then frozen at -80 °C. The cell pellets were resuspended in 20 mM sodium phosphate (pH 7.4), lysed with lysozyme (Sigma), and treated with benzonase nuclease (Sigma) to reduce the viscosity of the lysate. After stirring the lysate at rt for 30 min, NaCl was added to 0.5 M and imidazole was added to 20 mM. The lysate was clarified by centrifugation, and the supernatant was loaded onto a HisTrap nickel affinity column (GE Life Sciences) pre-equilibrated with 20 mM sodium phosphate (pH 7.4), 0.5 M NaCl, 20 mM imidazole. MBP was eluted from the column with 20 mM sodium phosphate (pH 7.4), 0.5 M NaCl, 500 mM imidazole. The eluate was concentrated and further purified by size-exclusion chromatography in PBS (HyClone) using a HiLoad 16/600 Superdex column (GE Life Sciences). Fractions containing pure protein (over 95% as indicated by SDS-PAGE) were pooled and concentrated. Protein concentration were determined from the absorbance at 280 nm using the extinction coefficient ε_{280} = 67 840 M^{-1} cm^{-1} calculated by the PROTPARAM server.[1] All MBP mutants were expressed and purified following the same procedure used for WT MBP. The concentrations of MBP(V293L) and MBP(V293A) were determined from the absorbance at 280 nm using the same extinction coefficient as WT MBP, and the extinction coefficient ε_{280} = 88 240 M^{-1} cm^{-1} was used for MBP(I329Y)-GFP.

Site-directed mutagenesis. Mutations were introduced to either the MBP or MBP(GFP) plasmid via site-directed mutagenesis using the forward and reverse primers listed in Table S3. The mutated plasmids were amplified in NEB-5α competent *E. coli* cells (New England Biolabs) and then purified using a miniprep kit (Qiagen). All mutated MBP genes were sequenced at University of Pennsylvania DNA Sequencing Facility to verify the incorporation of the desired mutation and the integrity of the gene sequence.

MBP-GFP cloning, expression, and purification. The gene encoding a "superfolder" variant of GFP[2] was amplified from the pET GFP LIC cloning vector, a gift from Scott Gradia acquired via

Addgene (plasmid #29772). The primers used for amplification are listed in Table S4. The GFP insert was added to the pET His6 MBP TEV LIC cloning vector by ligation independent cloning (LIC). The resulting MBP-GFP gene was sequenced at University of Pennsylvania DNA Sequencing Facility to verify the integrity of the fusion construct. MBP-GFP was expressed and purified following the same protocol used for MBP. Protein concentration were determined from the absorbance at 280 nm using the extinction coefficient ε_{280} = 86 875 M^{-1} cm^{-1}.

^{129}Xe hyper-CEST of purified MBP. ^{129}Xe was hyperpolarized and the z-spectra of MBP were acquired as described previously.[3] Briefly, hyperpolarized (hp) ^{129}Xe was generated using the spin-exchange optical pumping (SEOP) method with a home-built ^{129}Xe polarizer based on the IGI.Xe.2000 commercial model by GE. A Shark 65 W tunable ultra-narrow band diode laser (OptiGrate) set to 795 nm was used for optical pumping of Rb vapor. A gas mixture of 88% helium, 10% nitrogen, and 2% natural abundance xenon (Linde Group, NJ) was used as the hyperpolarizer input. ^{129}Xe hyperpolarization level was roughly 10-15%. For each data point in the hyper-CEST z-spectra, hp ^{129}Xe was bubbled into the NMR tube through capillaries for 20 s, followed by a 3-s delay to allow bubbles to collapse. A d-SNOB saturation pulse with 690 Hz bandwidth was used. Pulse length, t_{pulse} = 3.80 ms; field strength $B_{1,max}$ = 77 μT; number of pulses, n_{pulse} = 400; saturation time, T_{sat} = 1.52 s. NMR experiments were performed using a Bruker BioDRX 500 MHz NMR spectrometer and 10-mm PABBO probe, at 300 K. A 90° hard pulse of this probe has a pulse length of 22 μs. Unless otherwise noted, the protein concentration used was 80 μM, with 0.1% (v/v) Pluronic L81 (Aldrich) added to mitigate foaming. For the time-dependent saturation transfer experiments using 100 nM WT MBP, saturation frequencies of d-SNOB-shaped pulses were positioned +95 ppm and -95 ppm, referenced to the $Xe_{(aq)}$ peak, for on- and off-resonance, respectively. Pulse length, τ_{pulse} = 1.0496 ms; field strength, $B1_{max}$ = 279 μT. Both on-resonance and off-resonance data were fitted with first-order exponential decay curves. For the time-dependent saturation transfer experiments using 100 nM MBP(I329Y)-GFP, saturation frequencies of d-SNOB-shaped pulses were positioned +100 ppm and -100 ppm, referenced to the $Xe_{(aq)}$ peak, for on- and off-resonance, respectively. For the time-dependent saturation transfer experiments using 100 nM MBP(V293A), saturation frequencies of d-SNOB-shaped pulses were positioned +36 ppm and -36 ppm, referenced to the $Xe_{(aq)}$ peak, for on- and off-resonance, respectively.

^{129}Xe hyper-CEST of WT MBP-GFP in *E. coli*. BL21(DE3) *E. coli* competent cells were transformed with the WT MBP-GFP plasmid and cultured on a LB-agar plate supplemented with 50 μg/mL kanamycin. A single colony of transformed cells was used to inoculate 5 mL of LB medium supplemented with 50 μg/mL kanamycin. The 5 mL culture was incubated overnight at 37 °C with shaking at 250 rpm. The next morning the cells were pelleted and resuspended in 4 mL of minimal media. The resuspended cells were used to inoculate 4 x 1 L of minimal media supplemented with 50 μg/mL kanamycin in baffled culture flasks. Two flasks were supplemented with 1 mM maltose. The cell cultures were incubated at 37 °C with shaking at 250 rpm until OD_{600} reached ~1, at which point the two control flasks was stored at 4 °C and the other two flasks were induced by adding IPTG to a final concentration of 1 mM. The induced culture flasks were incubated overnight at 18 °C with shaking at 250 rpm and then stored at 4 °C. Aliquots from the control and induced cultures were centrifuged and the cell pellets were resuspended in PBS buffer with or without maltose. The concentrations of MBP-GFP in the IPTG-induced growths were measured by fluorescence spectroscopy (489 nm excitation; 510 nm emission) using a standard curve constructed from pure MBP-GFP in PBS. Cells were diluted so that the final MBP-GFP concentration was 1 μM. Cells from the control growths were diluted to match the optical densities (OD_{6oo}) of the induced cells. Saturation frequencies of d-SNOB-shaped pulses were positioned +95 ppm and -95 ppm, referenced to the $Xe_{(aq)}$ peak, for on- and off-resonance, respectively. Pulse length, τ_{pulse} = 1.0496 ms; field strength, $B1_{max}$ = 279 μT. Both on-resonance and off-resonance data were fitted with first-order exponential decay curves. Following hyper-CEST experiment, the cell samples were gently pelleted and the fluorescence of the extracellular solution was measured to check for cell lysis caused by xenon bubbling. 21% of the -maltose/+IPTG cells were lysed, and 18% of the +maltose/+IPTG cells were lysed.

CD spectroscopy and thermal stability measurements. The CD spectra of WT MBP, MBP V293L, and MBP V293A were measured on a Jasco J-1500 CD spectrometer equipped with a Peltier temperature controller. Spectra were acquired from 10 μM of protein in 10 mM sodium phosphate (pH 8.0) buffer inside a quartz cuvette with a 1-mm path length. CD spectra were taken at 20 °C with a wavelength step of 1 nm. CD spectra were performed in triplicate and averaged. Protein thermal stability was measured by increasing temperature from 20 to 90 °C. at a rate of 0.5 °C/min. Secondary structure was monitored at 222 nm with a step size of 1 °C and data integration time of 8 s. Thermal denaturation was repeated in triplicate, and melting

temperature (T_m) was calculated from the data using the *Spectra Analysis* tool in the J-1500 CD spectrometer software package (Jasco).

Fluorescence spectroscopy. Fluorescence spectroscopy was performed to evaluate maltose binding. Maltose binding to MBP results in quenched tryptophan fluorescence and produces a 2.5 nm red shift of the intrinsic fluorescence emission spectrum.[4-5] EPR spectroscopy of spin-labeled MBP showed that the red shift is indicative of MBP adopting a closed conformation.[6] The addition of maltose to V293L and V293A produced similar fluorescence quenching and red shifting as WT MBP, confirming maltose binding to the closed conformation. Fluorescence spectra were obtained on a Tecan Infinite M1000 PRO microplate reader using black 96 well flat-bottom microplates (Grenier Bio-One). MBP concentration was 4 μM in 20 mM HEPES (pH 7.4). Maltose was added to a final concentration of 400 μM and incubated with MBP for 15 min prior to measuring fluorescence. Excitation was at 280 nm and emission was scanned from 300 to 400 nm in 1 nm increments. All fluorescence assays were performed in triplicate and averaged. Fluorescence spectra were background corrected by subtracting the fluorescence spectrum of the well solution in the absence of protein.

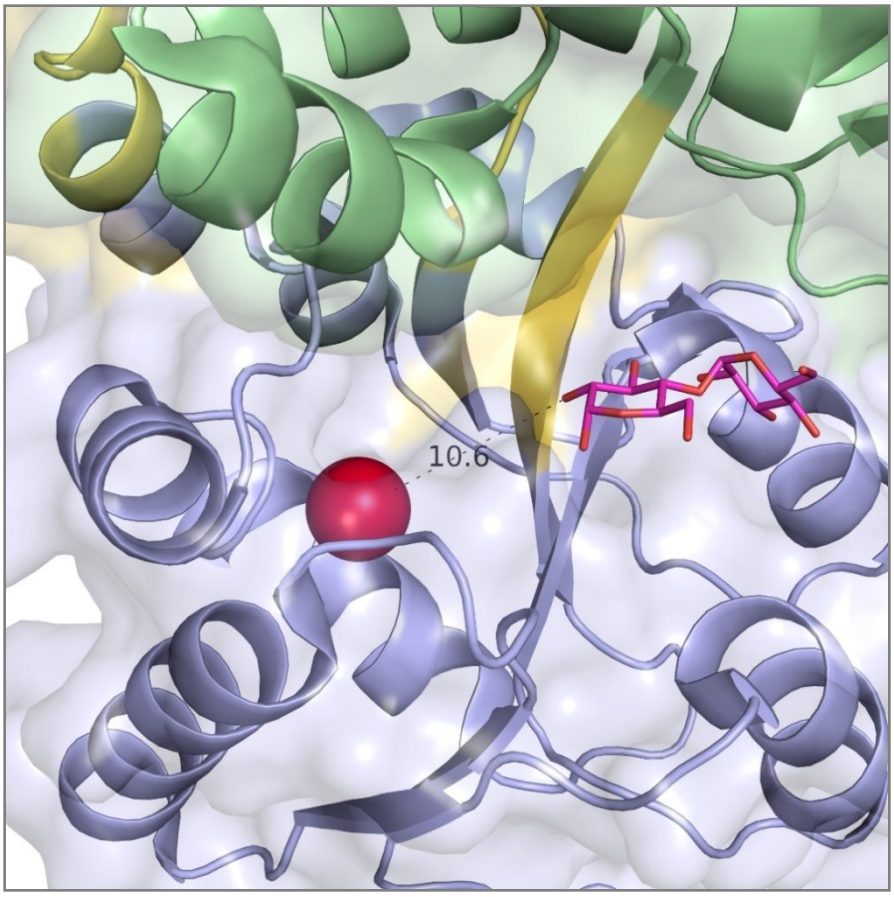

Figure S1. Model of maltose proximity to Xe-binding site. Maltose (purple sticks) bound to MBP_{closed} (PDB ID 1ANF)[7] overlaid onto the structure of MBP_{open} derivatized with Xe (PDB ID 1LLS).[8] Modelling was performed by aligning the N-terminal domains of the MBP_{open} and MBP_{closed} structures. Maltose is positioned 10.6 Å away from bound Xe.

Table S1. Peak widths (FWHM, in ppm) of hyper-CEST z-spectra

z-spectrum[a]	$Xe_{(aq)}$ peak (ppm)	Xe@MBP peak (ppm)	Xe@Bla peak (ppm)
PBS	1 ± 12	-	-
1 mM maltose	11.7 ± 0.9	-	-
80 μM MBP, no maltose	42 ± 2	-	-
80 μM MBP, 1 mM maltose	47 ± 2	35 ± 2	-
80 μM MBP(I329Y)-GFP, no maltose	53 ± 2	-	
80 μM MBP(I329Y)-GFP, 1 mM maltose	39 ± 2	34 ± 2	
27 μM MBP, 80 μM Bla, no maltose	52 ± 3	-	64 ± 7
27 μM MBP, 80 μM Bla, 1 mM maltose	53 ± 3	17 ± 5	86 ± 10
1 mM βCD	8.9 ± 0.7	-	-
80 μM MBP, 1 mM βCD	60 ± 2	-	-
80 μM MBP V293L, no maltose	19.1 ± 0.1	-	-
80 μM MBP V293L, 1 mM maltose	21.5 ± 0.9	-	-
80 μM MBP V293A, no maltose	37 ± 2	-	-
10 μM MBP V293A, 1 mM maltose	27 ± 2	20 ± 2	-
80 μM Bla[b]	47 ± 4	-	60 ± 7

[a] all spectra measured in PBS
[b] reported in ref. 3

(a)

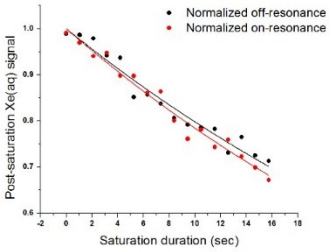
Normalized off-resonance
Normalized on-resonance
Post-saturation Xe(aq) signal
Saturation duration (sec)

(b)

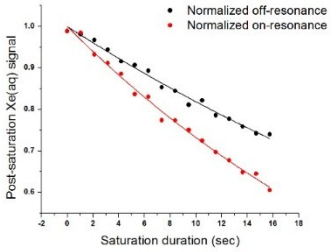
Normalized off-resonance
Normalized on-resonance
Post-saturation Xe(aq) signal
Saturation duration (sec)

(c)

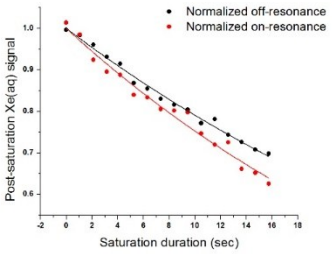
Normalized off-resonance
Normalized on-resonance
Post-saturation Xe(aq) signal
Saturation duration (sec)

(d)

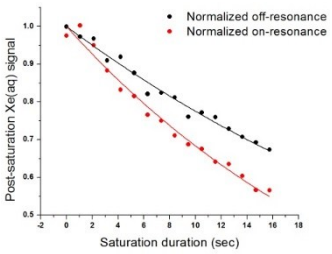
Normalized off-resonance
Normalized on-resonance
Post-saturation Xe(aq) signal
Saturation duration (sec)

(e)

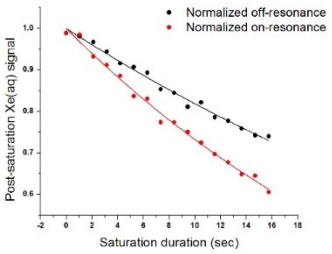
Normalized off-resonance
Normalized on-resonance
Post-saturation Xe(aq) signal
Saturation duration (sec)

(f)

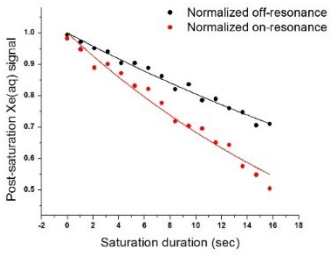
Normalized off-resonance
Normalized on-resonance
Post-saturation Xe(aq) signal
Saturation duration (sec)

(g)

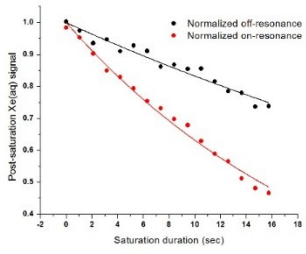
Normalized off-resonance
Normalized on-resonance
Post-saturation Xe(aq) signal
Saturation duration (sec)

Figure S2. Time-dependent saturation transfer data for 100 nM WT MBP at varying concentrations of maltose. (a) 0 μM maltose: saturation contrast = 0.022 ± 0.004; T_{1on} = 41 ± 2 s and T_{1off} = 44 ± 3 s. (b) 0.1 μM maltose: saturation contrast = 0.050 ± 0.007; T_{1on} = 34 ± 1 s and T_{1off} = 41 ± 3 s. (c) 0.3 μM maltose: saturation contrast = 0.05 ± 0.01; T_{1on} = 35 ± 1 s and T_{1off} = 43 ± 1 s. (d) 0.5 μM maltose: saturation contrast = 0.11 ± 0.01; T_{1on} = 26.3 ± 0.9 s and T_{1off} = 39 ± 1 s. (e) 1 μM maltose: saturation contrast = 0.118 ± 0.007; T_{1on} = 32.7 ± 0.7 s and T_{1off} = 50 ± 1 s. (f) 3 μM maltose: saturation contrast = 0.161 ± 0.004; T_{1on} = 26 ± 1 s and T_{1off} = 46 ± 2 s. (g) 1 mM maltose: saturation contrast = 0.26 ± 0.01; T_{1on} = 21.8 ± 0.7 s and T_{1off} = 55 ± 3 s. All measurements taken in pH 7.2 PBS at 300 K. Pulse length, τ_{pulse} = 1.0496 ms; field strength, $B_{1,max}$ = 279 μT. The number of pulses increased linearly from 0 to 15000.

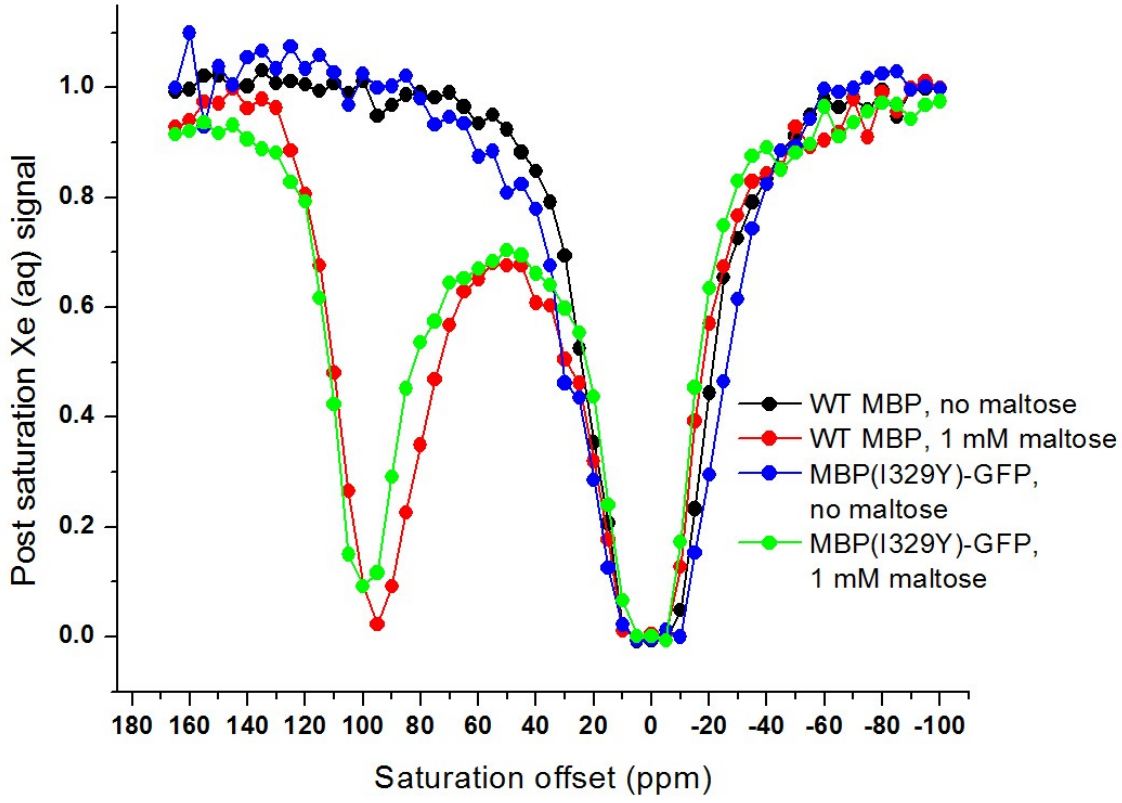

Figure S3. Comparison of CEST from WT MBP and MBP(I329Y)-GFP. Hyper-CEST z-spectra of 80 μM MBP(I329Y)-GFP with and without 1 mM maltose in pH 7.2 PBS at 300 K. The z-spectra of 80 μM WT MBP with and without 1 mM maltose shown for reference. Pulse length, τ_{pulse} = 3.8029 ms; field strength, $B_{1,max}$ = 77 μT.

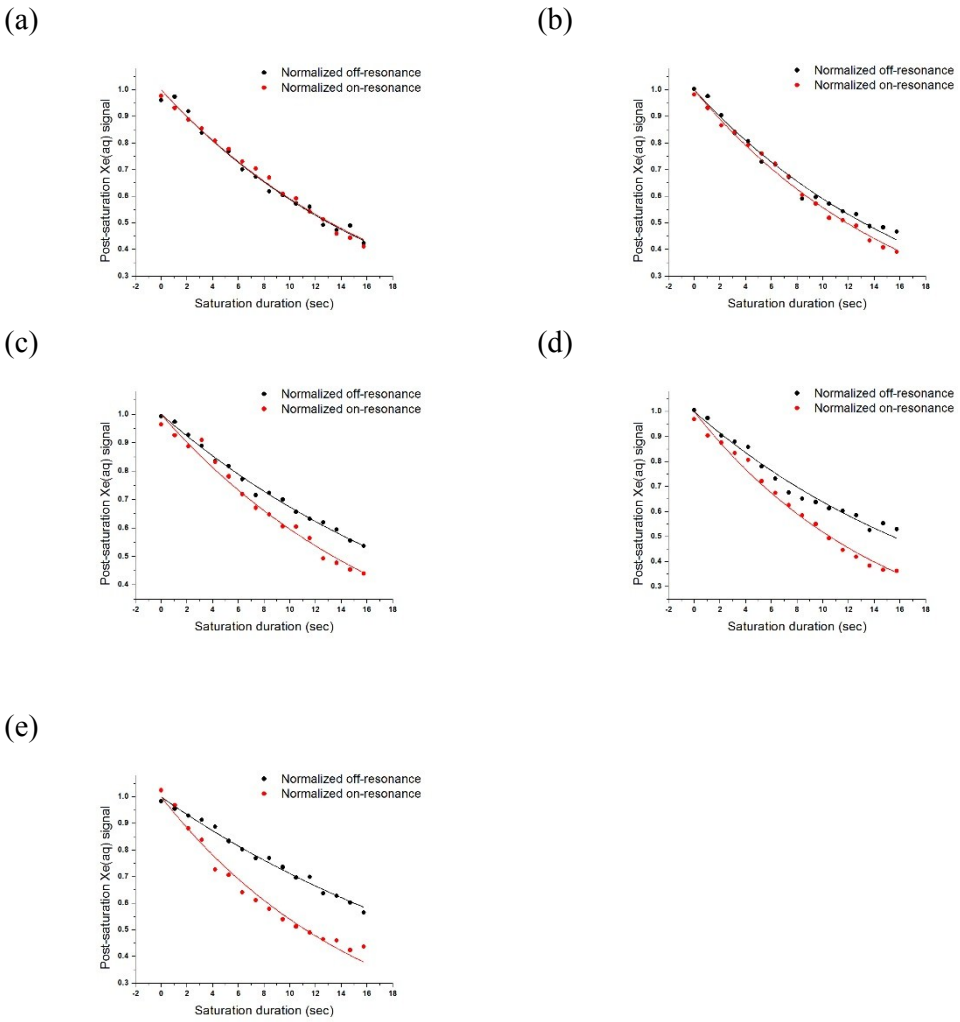

Figure S4. Time-dependent saturation transfer data for 100 nM MBP(I329Y)-GFP at varying concentrations of maltose. (a) 0 nM maltose: saturation contrast = 0.01 ± 0.01; T_{1on} = 19.0 ± 0.5 s and T_{1off} = 18.8 ± 0.6 s. (b) 32 nM maltose: saturation contrast = 0.07 ± 0.01; T_{1on} = 17.1 ± 0.4 s and T_{1off} = 19.0 ± 0.6 s. (c) 72 nM maltose: saturation contrast = 0.12 ± 0.02; T_{1on} = 19.3 ± 0.7 s and T_{1off} = 25.3 ± 0.6 s. (d) 140 nM maltose: saturation contrast = 0.173 ± 0.006; T_{1on} = 15.2 ± 0.5 s and T_{1off} = 22.3 ± 0.9 s. (e) 5 uM maltose: saturation contrast = 0.24 ± 0.01; T_{1on} = 16.2 ± 0.6 s and T_{1off} = 29.4 ± 0.8 s. All measurements taken in pH 7.2 PBS at 300 K. Pulse length, τ_{pulse} = 1.0496 ms; field strength, $B_{1,max}$ = 279 μT. The number of pulses increased linearly from 0 to 15000.

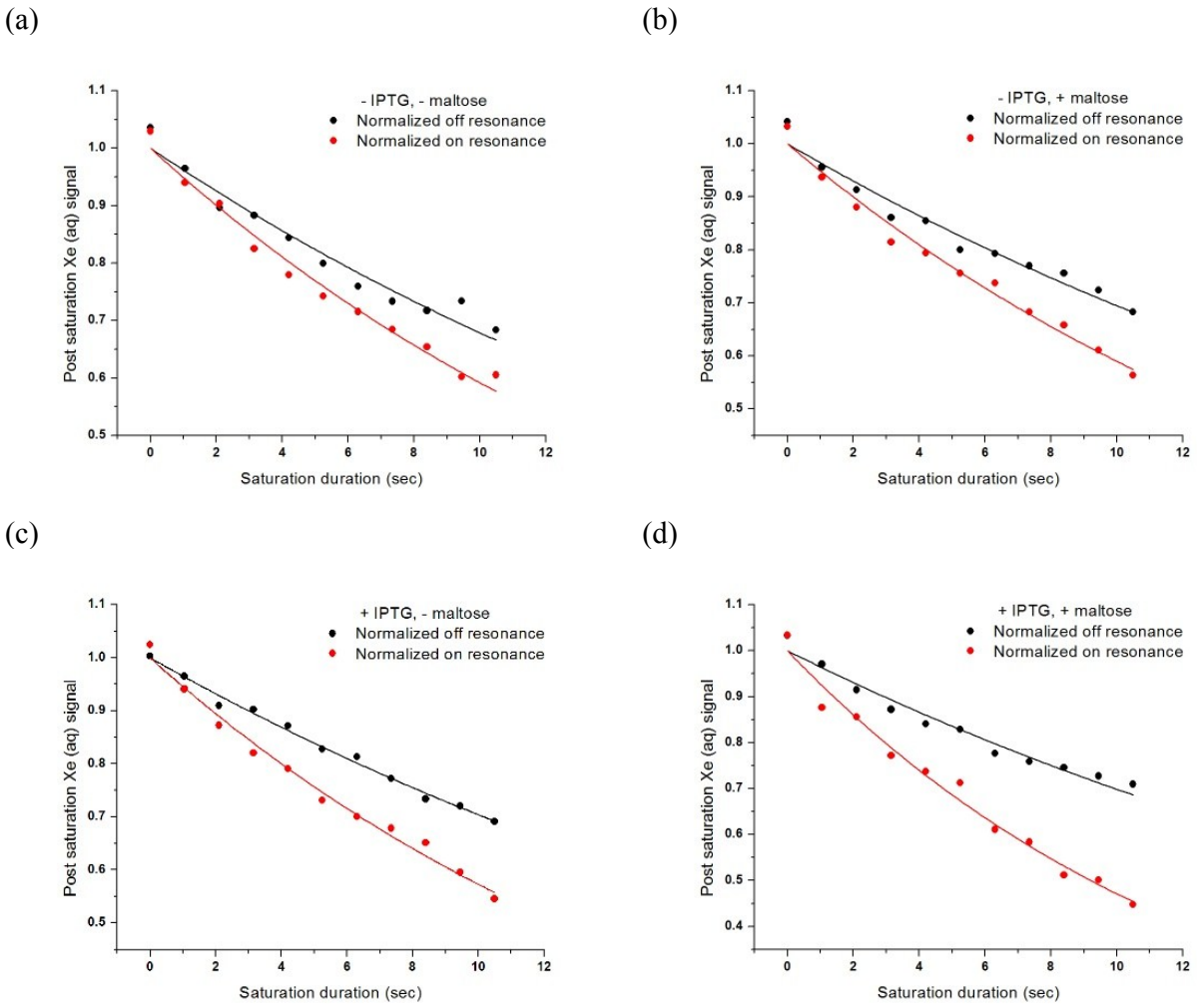

Figure S5. Time-dependent saturation transfer data for WT MBP-GFP in *E. coli*. (a) [MBP-GFP] < 0.001 μM, no maltose; saturation contrast = 0.09 ± 0.01 (b) [MBP-GFP] < 0.001 μM, 1 mM maltose; saturation contrast = 0.11 ± 0.01 (c) [MBP-GFP] = 1.0 ± 0.2 μM, no maltose; saturation contrast = 0.14 ± 0.01. (d) [MBP-GFP] = 1.00 ± 0.02 μM, 1 mM maltose; saturation contrast = 0.25 ± 0.02. All measurements taken in pH 7.2 PBS at 300 K. Pulse length, τ_{pulse} = 1.0496 ms; field strength, $B_{1,max}$ = 279 μT. The number of pulses increased linearly from 0 to 10000.

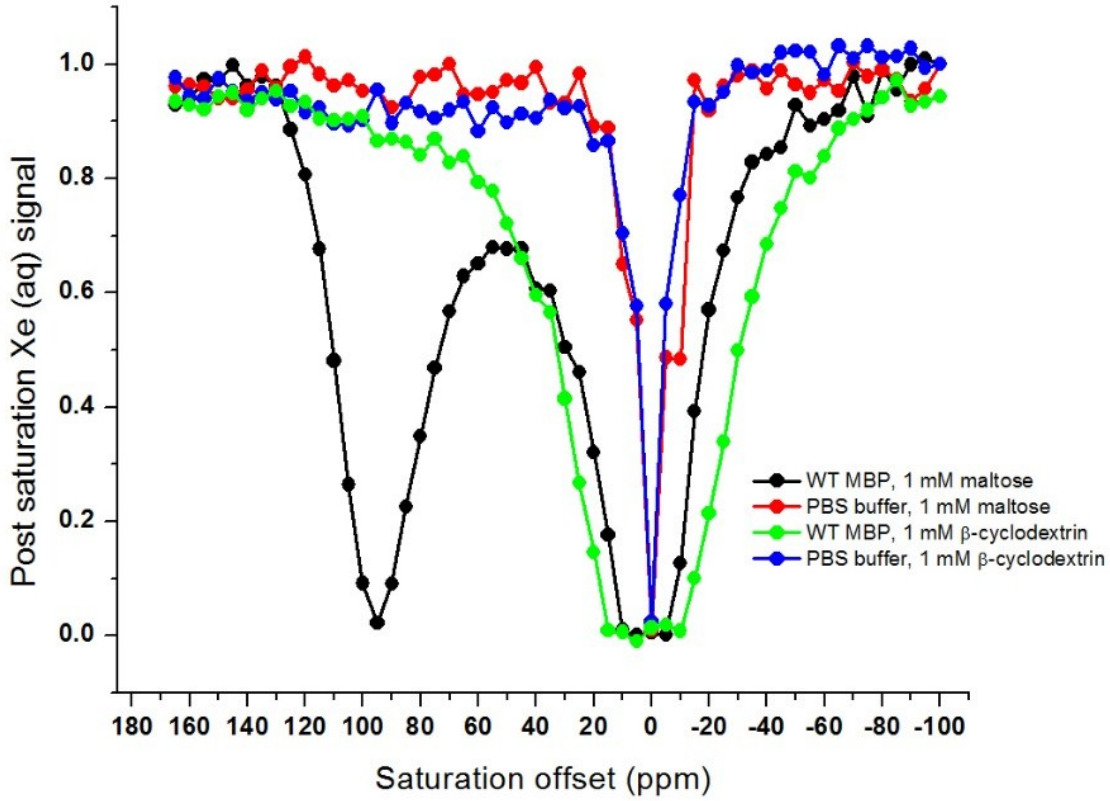

Figure S6. Comparison of CEST z-spectra from MBP with maltose or β-cyclodextrin. Hyper-CEST z-spectra of 80 μM WT MBP in the presence of 1 mM maltose and 1 mM β-cyclodextrin in pH 7.2 PBS at 300 K. The z-spectra of 1 mM maltose and 1 mM β-cyclodextrin in the absence of MBP are shown for reference. Pulse length, τ_{pulse} = 3.8029 ms; field strength, $B_{1,max}$ = 77 μT.

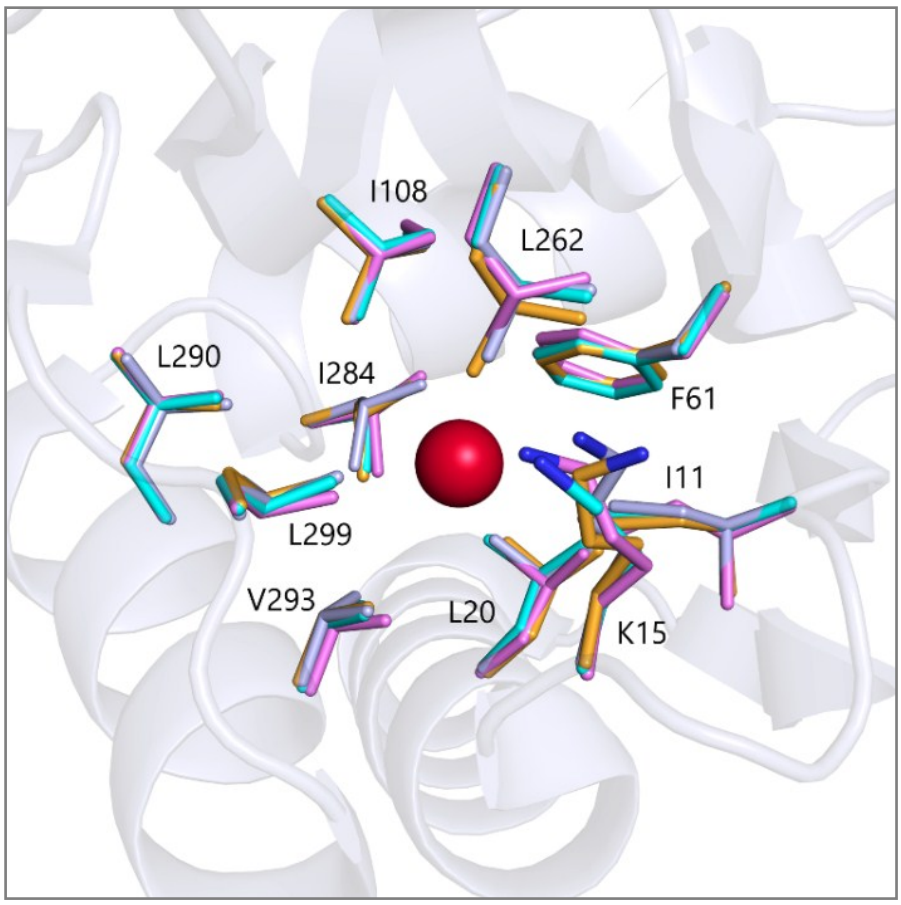

Figure S7. Comparison of the Xe-binding pocket in multiple MBP crystal structures. The conformations of the hydrophobic residues lining the pocket are conserved among MBP_{open} (cyan; PDB ID 1OMP),[9] MBP_{open} derivatized with Xe (light blue; PDB ID 1LLS),[8] MBP_{open} bound to βCD (violet; PDB ID 1DMB),[10] and MBP_{closed} bound to maltose (orange; PDB ID 1ANF).[7] There is slight variation, though, in the position of the terminal amine of Lys-15.

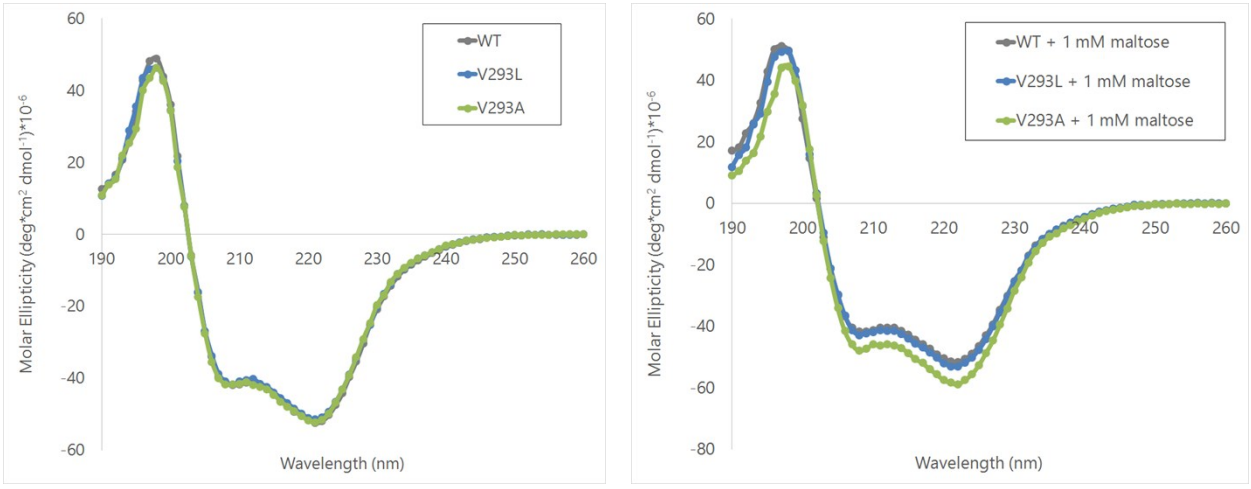

Figure S8. CD spectra of MBP(V293L) and MBP(V293A). 10 μM MBP without maltose (left) and with 1 mM maltose (right) in 10 mM sodium phosphate buffer (pH 8.0).

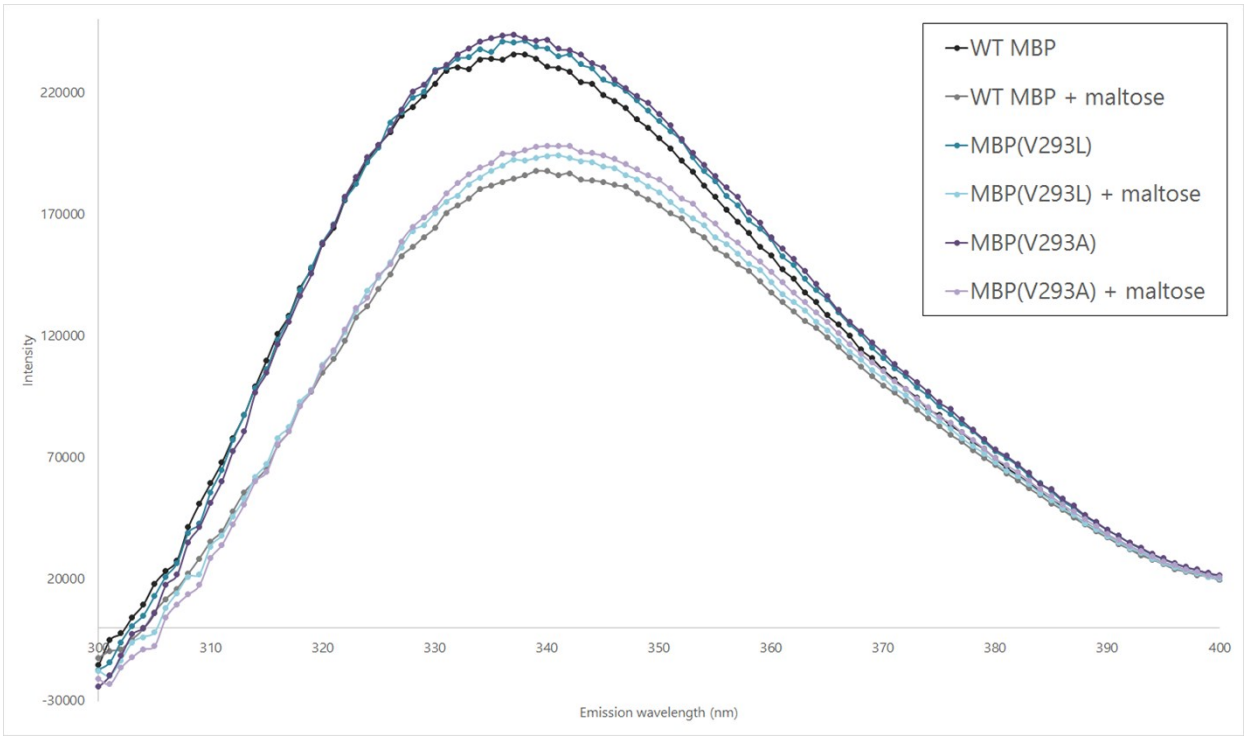

Figure S9. Fluorescence spectra of MBP(V293L) and MBP(V293A). Spectra show the quenching of fluorescence upon maltose binding. The magnitude of fluorescence quenching was roughly equal among WT MBP (22%), MBP V293L (20%), MBP V293A (20%). The addition of maltose red-shifted the maximum emission wavelengths of all MBP proteins by 2-3 nm, indicating the transition from open to closed conformation upon ligand binding.

Table S2. Thermal stabilities of MBP(V293L) and MBP(V293A)

Protein	T_m (°C)[a]
WT MBP	53.9 ± 0.7
WT MTP + 1 mM maltose	61.0 ± 0.8
MBP-V293L	53.8 ± 0.8
MBP-V293L + 1 mM maltose	59.5 ± 0.9
MBP-V293A	50.1 ± 0.7
MBP-V293A + 1 mM maltose	55.7 ± 0.7

[a] Data reported as mean ± standard deviation (n=3)

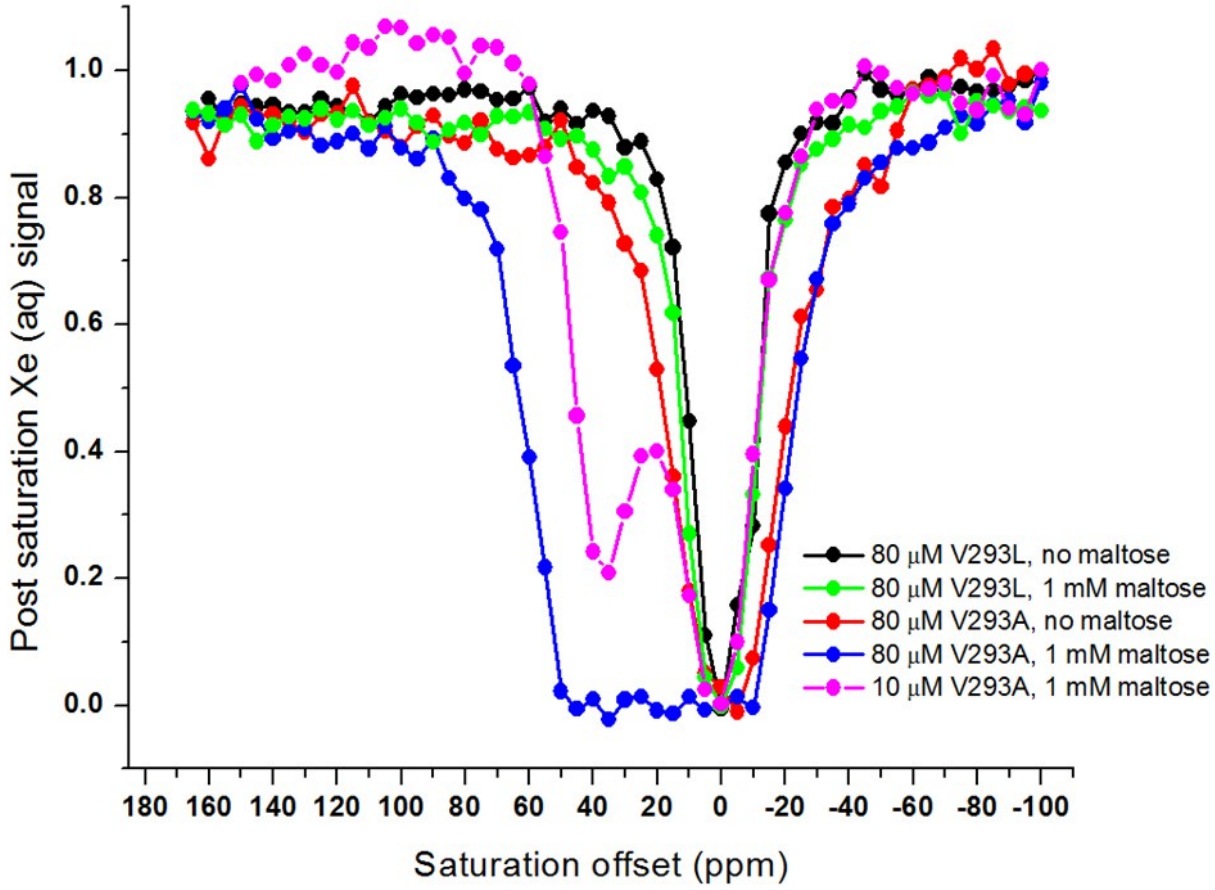

Figure S10. Hyper-CEST z-spectra from MBP(V293L) and MBP(V293A). Hyper-CEST z-spectra of 80 μM MBP(V293L) with and without 1 mM maltose, 80 μM MBP(V293A) with and without 1 mM maltose, and 10 μM MBP(V293A) with 1 mM maltose. All measurements taken in pH 7.2 PBS at 300 K. Pulse length, τ_{pulse} = 3.8029 ms; field strength, $B_{1,max}$ = 77 μT.

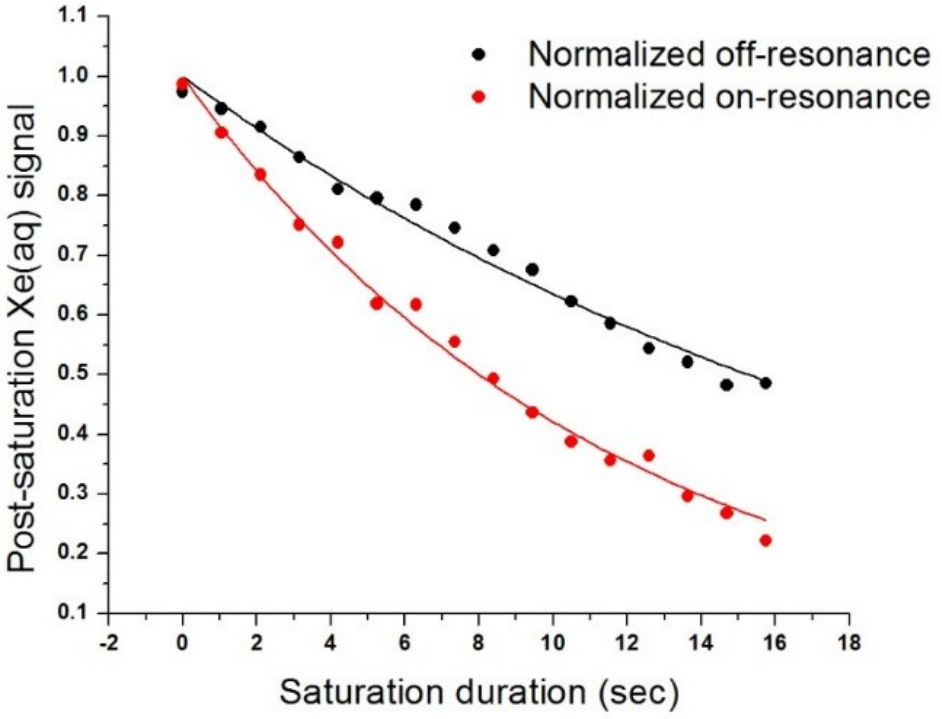

Figure S11. Time-dependent saturation transfer data for 100 nM MBP(V293A). The observed saturation contrast is 0.35 ± 0.02. Saturation frequencies of d-SNOB-shaped pulses were positioned +36 ppm and -36 ppm, referenced to the $Xe_{(aq)}$ peak, for on- and off-resonance, respectively. Pulse length, τ_{pulse} = 1.0496 ms; field strength, $B1_{max}$ = 279 μT. Both on-resonance and off-resonance data were fitted with first-order exponential decay curves, with T_{1on} = 11.6 ± 0.3 s and T_{1off} = 22.0 ± 0.7 s. Measurements taken in pH 7.2 PBS at 300 K. Pulse length, τ_{pulse} = 1.0496 ms; field strength, $B_{1,max}$ = 279 μT. The number of pulses increased linearly from 0 to 15000.

Table S3. Oligonucleotide primers used in site-directed mutagenesis

V293L	Forward primer	5′– GAAGGTCTGGAAGCGCTGAATAAAGACAAACCG –3′
	Reverse primer	5′– CGGTTTGTCTTTATTCAGCGCTTCCAGACCTTC –3′
V293A	Forward primer	5′– GAAGGTCTGGAAGCGGCGAATAAAGACAAACCG –3′
	Reverse primer	5′– CGGTTTGTCTTTATTCGCCGCTTCCAGACCTTC –3′
I329Y	Forward primer	5′– CGCCCAGAAAGGTGAATACATGCCGAACATCCCGC –3′
	Reverse primer	5′– GCGGGATGTTCGGCATGTATTCACCTTTCTGGGCG –3′

Table S4. Oligonucleotide primers used for GFP insert amplification

GFP insert	Forward primer	5′– TACTTCCAATCCAATGCAAGCAAGGGCGAGGAGCTGTTC –3′
	Reverse primer	5′– TTATCCACTTCCAATGTTATTACTTGTACAGCTCGTCCATGCC –3′

References

(1) Gasteiger, E., Hoogland, C., Gattiker, A., Duvaud, S., Wilkins, M. R., Appel, R. D., and Bairoch, A. In *The Proteomics Protocols Handbook*; Walker, J. M., Ed.; Humana Press: Totowa, **2005**; pp 571− 607.

(2) Pédelacq, J.-D.; Cabantous, S.; Tran, T.; Terwilliger, T. C.; Waldo, G. S. *Nat. Biotechnol.* **2006**, *24*, 79–88.

(3) Wang, Y.; Roose, B. W.; Palovcak, E. J.; Carnevale, V.; Dmochowski, I. J. *Angew. Chemie Int. Ed.* **2016**, *55*, 8984– 8987.

(4) Szmelcman, S.; Schwartz, M.; Silhavy, T. J.; Boos, W. *Eur. J. Biochem.* **1976**, *65*, 13–19.

(5) Hall, J. A; Gehring, K.; Nikaido, H. *J. Biol. Chem.* **1997**, *272*, 17605–17609.

(6) Hall, J. A; Thorgeirsson, T. E.; Liu, J.; Shin, Y. K.; Nikaido, H. *J. Biol. Chem.* **1997**, *272*, 17610–17614.

(7) Quiocho, F. A.; Spurlino, J. C.; Rodseth, L. E. *Structure* **1997**, *5*, 997–1015.

(8) Rubin, S. M.; Lee, S. Y.; Ruiz, E. J.; Pines, A.; Wemmer, D. E. *J. Mol. Biol.* **2002**, *322*, 425–440.

(9) Sharff, A. J.; Rodseth, L. E.; Spurlino, J. C.; Quiocho, F. A. *Biochemistry* **1992**, *31*, 10657–10663.

(10) Sharff, A J.; Rodseth, L. E.; Quiocho, F. A. *Biochemistry* **1993**, *32*, 10553–10559.